AIAA JOURNAL
Vol. 34, No. 8, August 1996

Aeroacoustic Properties of a Supersonic Diamond-Shaped Jet

F. S. Alvi,* A. Krothapalli,† D. Washington,‡ and C. J. King‡
Florida A&M University and Florida State University, Tallahassee, Florida 32316-2175

The potential for using a novel diamond-shaped nozzle, which may allow superior mixing and noise characteristics of supersonic jets without significant thrust losses, is explored. Flow visualization and pressure measurements indicate the presence of distinct structures in the shear layers, not normally observed in shear layers of ideally expanded axisymmetric and rectangular jets. The characteristics of these features suggest that they are a manifestation of significant streamwise vorticity in the shear layers. Despite the distinct nature of the flowfield structure of the diamond jet, the far-field noise characteristics are quite similar to those of the corresponding axisymmetric jet, except moderate mixing-noise reduction in the aft quadrant. Furthermore, the global shear-layer growth rates are also very similar to those of the axisymmetric and two-dimensional counterparts. These observations lead one to believe that the presence of streamwise vorticity may not play a significant role on the overall mixing and noise generation of a supersonic jet.

I. Introduction

STEALTH capabilities of modern fighter aircraft require the use of complex nozzle geometries such as the one considered here. These nozzles generally provide a reduced radar signature as well as a much reduced infrared (IR) signature. The reduction in IR signature is attributed to the enhanced mixing of hot gases with the colder ambient air, which generally will result in reduced far-field noise. However, the detailed flow and acoustic characteristics of jets issuing from these nozzles are not yet available. This paper provides the basic properties of a jet issuing from a converging–diverging diamond-shaped nozzle, a representative of a stealth nozzle. The noise characteristics of such a jet also may prove to be beneficial for the High Speed Civil Transport application.

An admirable review of supersonic jet noise was recently provided by Tam.[1,2] The principal components of the supersonic jet noise are turbulent mixing noise, which includes Mach wave radiation, broadband shock-associated noise (for overexpanded/underexpanded jets), and screech tones. The turbulent mixing noise of a perfectly expanded jet is largely determined by the behavior of compressible shear layers, within the first few diameters of the nozzle exit. A number of studies have afforded considerable insight into the behavior of two-dimensional compressible shear layers.[3–6]

For the jet operating conditions considered here, where the convective Mach number M_c is greater than 0.8 [$M_c = (U_1 - U_2)/(a_1 + a_2)$, where U_1 and U_2 denote the freestream velocities in the high- and low-speed streams, respectively, and a_1 and a_2 represent the acoustic velocities in the two freestreams[4]], the shear layers are expected to display three-dimensionality with little evidence of large-scale organized structures.[5] In addition, noncircular nozzles that possess corners tend to generate significant streamwise vorticity, which may potentially enhance mixing. Various investigators have attempted to enhance the diffusion of supersonic jets through the generation of streamwise vorticity. Among the more frequently used techniques is the modification of the nozzle exit geometry by placing tabs or cutting slots at the exit plane of the nozzle. Although the mixing characteristics of these vorticity-added jets has demonstrated moderate improvement, the effect of the vorticity on the far-field noise is still an unresolved issue (see Krothapalli et al.[7] and the references therein).

The studies of Hawkins and Hoch[8] and Pannu and Johannesen,[9] who investigated the flowfield generated by notched axisymmetric nozzles, were among the earliest on the effect of streamwise vorticity on jet noise. They discovered that strong streamwise vortices produced by the notches reduced the sideline noise significantly by essentially redirecting it in the longitudinal direction. In contrast, a recent study revealed that although screech tones and shock-associated noise were reduced by the addition of moderate streamwise vorticity, the increase in the turbulent mixing noise resulted in an insignificant effect on the overall far-field noise for axisymmetric jets.[7] Those findings suggest that for ideally expanded jets, where no waves are present, the addition of streamwise vorticity may even lead to an increase in the jet noise. In the present study, it was expected that the sharp corners of the diamond nozzle would lead to the creation of significant streamwise vorticity and, subsequently, to a modification of the mixing and acoustic properties of the jet.

The geometry of the nozzle also determines the degree of frictional losses and the resulting thrust loss. Higher nozzle area-to-perimeter ratios lead to lower frictional losses, making the axisymmetric nozzle the most efficient in this context. In contrast, a rectangular nozzle will have the highest frictional loss, whereas the diamond shape falls somewhere between the two geometries. The compromise in the thrust loss, together with the expected improved stealth and mixing characteristics, make the diamond nozzle an attractive choice for further exploration. Furthermore, a technique called fluidic thrust vectoring, which utilizes counterflow to redirect the jet thrust,[10] is more easily and effectively applied to noncircular geometries, adding further impetus for the study of this nozzle. The present goal was to conduct a detailed, fundamental study of the flowfield and noise properties of a Mach 2 ideally expanded diamond-shaped jet issuing from a converging–diverging (C–D) nozzle.

II. Apparatus and Procedures

A. Diamond Nozzle

A Mach 2, stainless steel, C–D, diamond-shaped nozzle was fabricated using an electric discharge machining (EDM) technique that provided a surface finish quality of better than 30 μm (0.0004 in.). The initially round converging section of the nozzle smoothly transitions to a diamond shape (aspect ratio = 2) at the nozzle throat. The diamond cross-section is maintained as the walls diverge at an angle of 3 deg from the throat to the nozzle exit. The exit area was picked such that it matched the exit areas of axisymmetric and rectangular (aspect ratio = 4) Mach 2 C–D nozzles, which have been extensively investigated and whose behavior has been well-documented (the rectangular nozzle used for comparison has straight side walls

Received May 13, 1995; presented as Paper 95-169 at the AIAA/CEAS 1st Joint Aeroacoustics Conference, Munich, Germany, June 12–15, 1995; revision received April 23, 1996; accepted for publication April 24, 1996.

*Assistant Professor, Fluid Mechanics Research Laboratory, Department of Mechanical Engineering. Member AIAA.

†Don Fuqua Professor, Departmental Chairman, Fluid Mechanics Research Laboratory, Department of Mechanical Engineering. Associate Fellow AIAA.

‡Graduate Research Assistant, Fluid Mechanics Research Laboratory, Department of Mechanical Engineering.

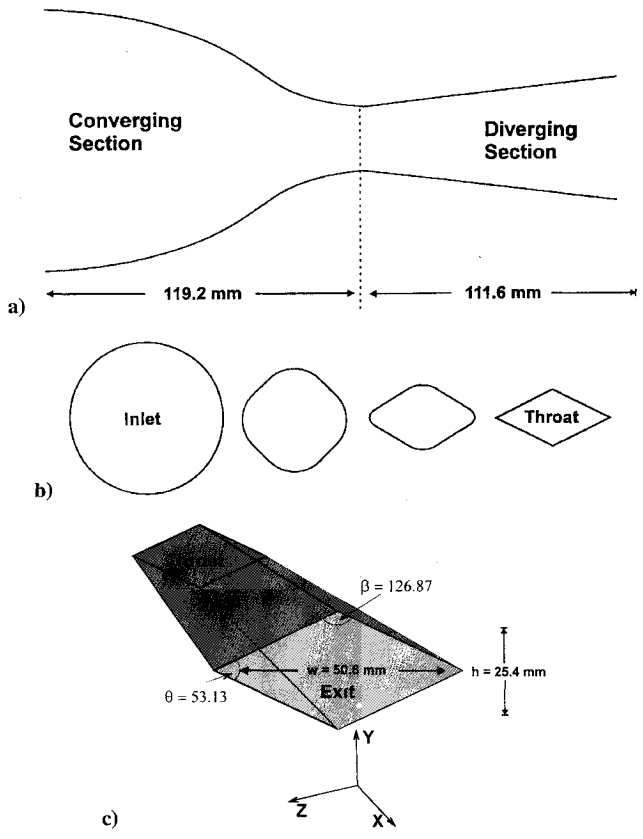

Fig. 1 Diamond nozzle.

and is C–D only in short dimension). Figure 1a shows a side view of the diamond nozzle, and Fig. 1b depicts the converging section of the nozzle where transition from a circular inlet (diameter = 57 mm) to the diamond-shaped throat takes place. The pseudoisometric view shown in Fig. 1c illustrates the diverging section of the nozzle. The high-pressure dry air needed to create the jet is supplied by a bank of storage tanks (total capacity 10 m^3) that are normally pressurized to 13.8 MPa.

B. Measurement and Analysis Techniques

A conventional pitot probe with a circular opening of 0.69 mm (0.027 in.) was used for the surveys. The probe is traversed using a high-resolution, three-axis, indexer/stepper motor with a step size of 0.0127 mm (0.0005 in.) allowing for detailed pitot surveys. A Lumonics Nd:YAG laser with a pulse duration of 10–12 ns (400 mJ/pulse, 20-Hz repetition rate) was used to generate a very thin, very bright light sheet for the planar laser scattering (PLS) flow visualization study. The shear layers were rendered visible by the extremely small condensation droplets formed as a result of the mixing of the cold jet flow with the relatively moist ambient air. A conventional schlieren system was used to visualize the jet and the accompanying near sound field. The PLS images were recorded using a Kodak MegaPlus, Model 4.2 digital camera with a resolution of 2048 × 2048 pixels. PLS imagery also was recorded on S-VHS videotape (standard 30-Hz framing rate) using a Panasonic high-resolution (512 × 480 pixels) charge-coupled device video camera.

The acoustic data were obtained in the anechoic chamber pictured schematically in Fig. 2. To simulate aircraft takeoff and landing conditions, the chamber was built to enclose the open-jet portion of the low-speed closed-return wind tunnel as well as the supersonic jet depicted in the figure. The low-speed wind tunnel provides a 61 × 61-cm jet of air surrounding the supersonic jet, with a maximum velocity of approximately 60 m/s. The exit of the coflowing jet was blocked in this experiment; hence the supersonic jet was issuing into quiescent air. Where possible, all surfaces in the room were covered with 10.2-cm wedge-shaped sound-absorbing foam. The chamber satisfied anechoic conditions at frequencies of 500 Hz and above.

The measurements were made using a single B&K 6.35-mm free-field microphone that could be moved to any point in the shaded region of the schematic via a two-dimensional traverse. The location of microphone relative to the jet centerline is defined by the angle θ, depicted in Fig. 2. The microphone remained perpendicular to the jet axis throughout the experiments. (In principle, free-field microphones are insensitive to diaphragm orientation for far-field acoustic measurements.) To ensure a flat response (±1 dB) up to 100 kHz, the protective grid was removed from the microphone. It was calibrated periodically, and the calibration varied less than 0.5 dB over the length of the experiment. All sound pressure level data are presented in dB relative to 20 μPa.

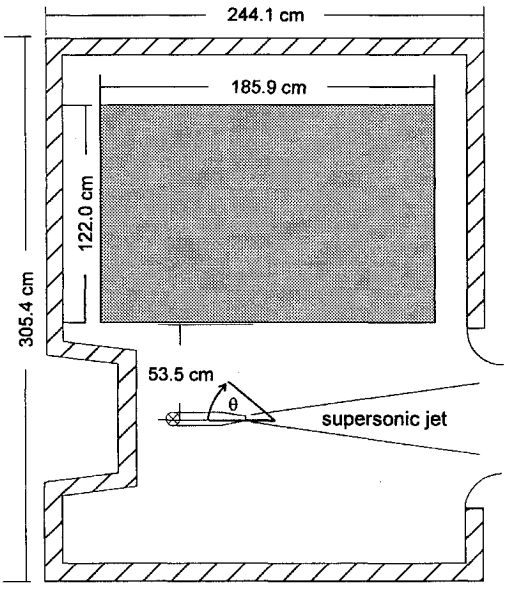

Fig. 2 Anechoic facility.

At each data location, 102,400 points were recorded at a sampling rate of 250 kHz with a cutoff frequency of 100 kHz. Standard statistical analysis techniques were used to obtain the spectral content and the overall sound pressure level (OASPL) from these measurements. Each data record was segmented into 100 groups with 1024 points each, and a fast Fourier transform (FFT) with a frequency resolution of 244.1 Hz was computed for each segment. The 100 FFTs thus obtained were averaged to obtain a statistically reliable estimate of the narrow-band noise spectrum, from which the OASPL was calculated.

III. Results and Discussion

A. Flow Visualization

The nature of the jet shear layers, with a convective Mach number M_c of approximately 0.84, was first qualitatively explored via the PLS technique. Side views of the shear layers, obtained by slicing the flowfield along the jet centerline with a planar laser sheet, are shown in Fig. 3. Each image is exposed by a single laser pulse, thus essentially freezing the structure. Three different orientations of the light sheet, two parallel to the minor and major axes (Figs. 3a and 3b, respectively) and one parallel to one of the nozzle edges (not shown), were used to completely characterize the streamwise development of the shear layer. The inset in each image indicates the relative orientation of the light sheet.

Shear layers visualized in these images extend from the nozzle exit to $x/h \approx 14$, h being the nozzle short dimension (see Fig. 1). These shear layers always appear brighter in the center of the image because the beam waist falls in this region. Large-scale, steeply inclined structures are clearly visible in these images. Qualitatively speaking, these structures appear to be somewhat larger when compared to axisymmetric shear layers at comparable compressibility. An examination of multiple instantaneous images reveals that the large structures begin to penetrate beyond the jet centerline at streamwise distances of $x/h \approx 7.5$, suggesting that the jet potential core ends at approximately this location.

Quantitative information regarding the visual growth rates of the shear layers also was obtained from time-averaged PLS images (not

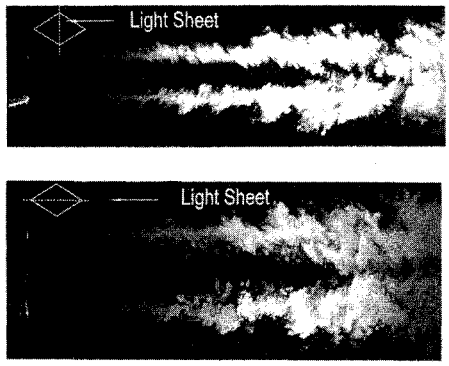

Fig. 3 Instantaneous PLS images, side views.

shown here). To compare the measured visual growth rate, $d\delta_{vis}/dx$, with the compressible-shear-layer data in the literature, the visual growth rate was converted to a pitot growth rate, $d\delta_{pit}/dx$ via a scaling factor of 0.72 (Ref. 4) and normalized by the corresponding incompressible growth rate. The normalized growth rate was measured to be 0.37 and agrees very well with the $M_c \approx 0.82$ axisymmetric shear-layer measurements of Strykowski and Krothapalli,[10] where similar PLS images were used for this measurement. The agreement with axisymmetric shear-layer data suggests that the different shear-layer dynamics of axisymmetric and diamond-shaped jets result in a very similar growth rate; a somewhat unexpected result.

Diametral or cross-sectional views of the flowfield (in the y–z plane) also were obtained at various streamwise locations. Figure 4 shows a series of such instantaneous PLS images at four streamwise locations. The most striking feature in these images is the presence of several corrugated structures along the edges of the shear layer. These structures bear a marked resemblance to the streamwise vortical structures observed by Krothapalli et al.[11] (see references therein) and Arnette et al.[12] in axisymmetric, underexpanded supersonic jets. In addition to the corrugated structures, presence of larger structures at the jet vertices is also evident. In the jet near field (Figs. 4a and 4b), the corrugated structures (at the jet sides) and the larger structures (in the jet corners) are approximately the same size. As one progresses farther downstream to $x/h = 6$ (Fig. 4c), the features at the corners dominate the overall flowfield, distorting the potential core and penetrating near the jet centerline. By the time one reaches $x/h = 12$ (Fig. 4d), the potential core disappears entirely and the corner structures are the only distinguishable features.

An examination of multiple instantaneous PLS images, similar to those shown in Fig. 4, substantiates the spatially stationary nature of these structures. A discussion of the origin, behavior, and significance of these structures is delayed until the results of the pitot measurement have been presented. At this juncture we merely note that the appearance of such distinct structures, usually not observed in highly compressible shear layers of ideally expanded axisymmetric and two-dimensional supersonic jets, and their resemblance to previously observed streamwise structures[11,12] suggests that these features are a manifestation of significant streamwise vorticity.

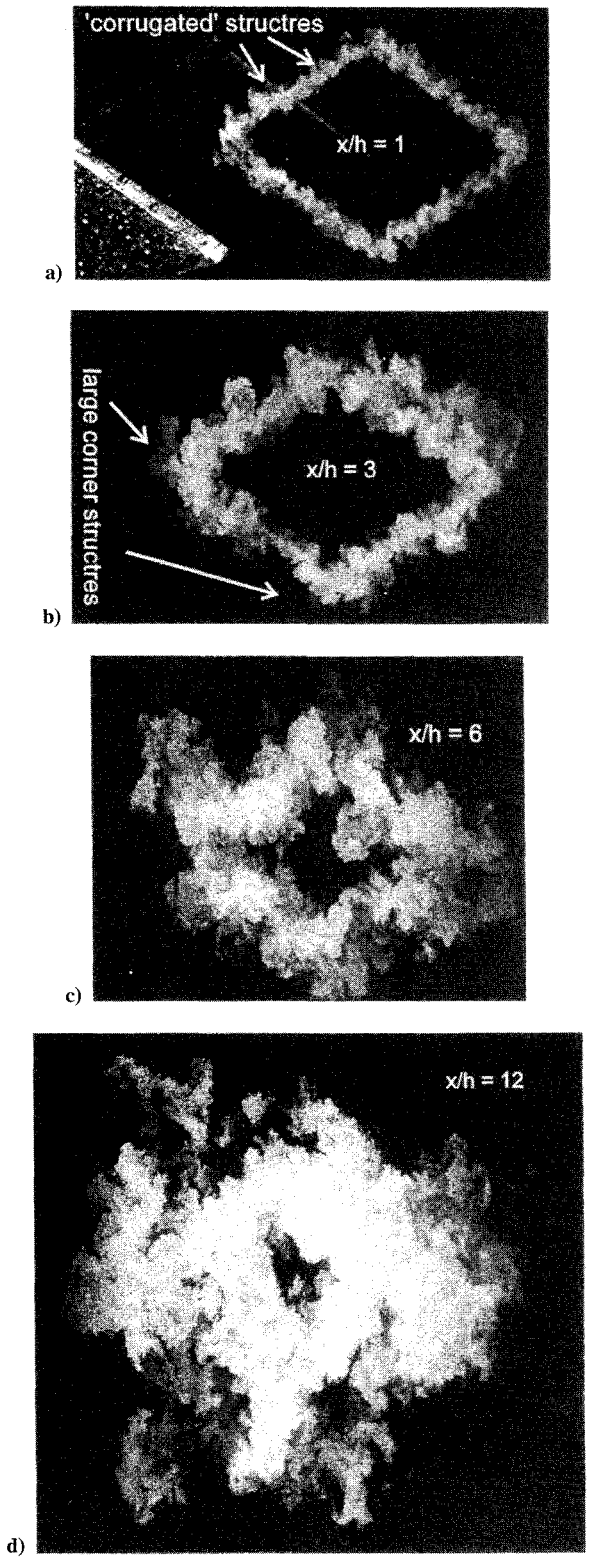

Fig. 4 Instantaneous PLS images, cross-sectional views.

B. Centerline Pitot Surveys

Centerline pitot surveys were conducted to determine the extent of the potential core of this Mach 2.0 diamond jet. A comparison of the centerline axial Mach profile of a diamond jet with axisymmetric and rectangular jets is plotted in Fig. 5. (Mach number was calculated using the measured pitot pressures and assuming that static pressure is equal to ambient pressure.) For such a comparison to be physically realistic, it is essential that the streamwise coordinate x be nondimensionalized with an appropriate length scale. However, because of the large disparity in the geometry of the three types of jets, a proper choice of the length scale is not trivial.

In this plot, an equivalent diameter is used to nondimensionalize the streamwise distance. The equivalent diameter, D_{eq} is calculated by equating the area of the actual nozzle to that of a hypothetical circular nozzle with a diameter D_{eq}. This choice seems to be the most appropriate for the following reasons. First, as we mentioned earlier, the diamond, rectangular, and axisymmetric nozzles all have the same exit areas, hence the same D_{eq}. Second, this length-scale concept has been successfully used for comparing data between circular and rectangular jets with equal exit areas but different geometries. We also must provide a word of caution: For rectangular nozzles with high aspect ratios (generally greater than 4), the suitability of using the equivalent diameter becomes questionable. Because the rectangular nozzle, whose data are shown in Fig. 5, has an aspect ratio of 4 one must view this comparison with caution. Nonetheless,

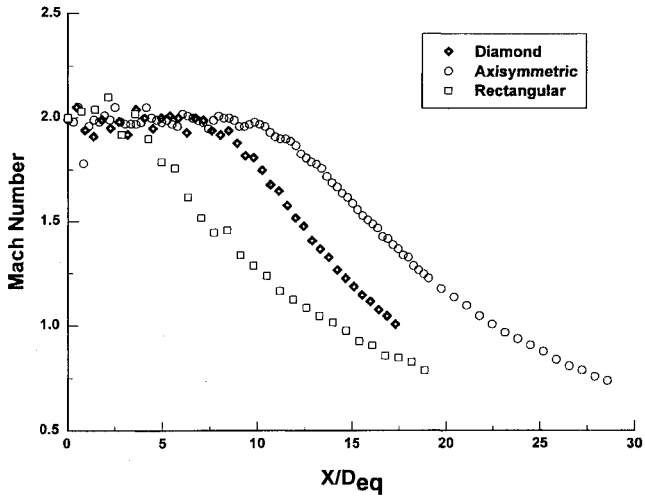

Fig. 5 Axial centerline Mach profile.

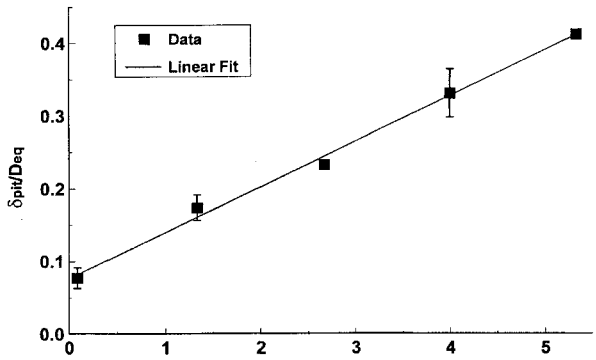

Fig. 6 Streamwise growth of shear layer.

for the sake of completeness and to provide some qualitative insight, the rectangular nozzle data are shown in Fig. 5. In this nondimensionalized space, the rectangular jet has the shortest potential core and the axisymmetric jet has the longest, whereas the diamond jet is between the two.

C. Shear-Layer Growth Rates

Though the relative lengths of the potential cores yield some insight into the mixing behavior of the three different types of shear layers, our caveat regarding the appropriateness of D_{eq}, especially for rectangular nozzles, makes such a comparison somewhat qualitative. To obtain a more reliable estimate of the shear-layer growth, detailed pitot surveys across the shear layer also were conducted at several streamwise locations. At each location, the shear-layer pitot thickness δ_{pit} was estimated using the well-known criterion of $0.05\Delta P_{pit} - 0.95\Delta P_{pit}$ (Ref. 4). A plot of the nondimensional shear-layer thickness, δ_{pit}/D_{eq}, as a function of nondimensional streamwise distance, is shown in Fig. 6. The estimated uncertainty at points for which error bars are not shown is less than the symbol size.

The growth rate, $\delta' = d\delta_{pit}/dx$, estimated from a linear fit to the data and normalized by the corresponding incompressible value (δ'_0), was measured as 0.27. To place the present measurements in perspective, the normalized growth rates, δ'/δ'_0, obtained directly from pitot measurements and converted from visual growth rates, are plotted in Fig. 7 along with similar measurements obtained by various investigators over a broad compressibility range. The present measurements lie well within the scatter of previously published data and agree with measurements of axisymmetric and two-dimensional shear layers at comparable M_c. This agreement suggests that the presence of streamwise vorticity, at least at the levels present in this study, may not affect the global entrainment properties of compressible shear layers.

One final note regarding the growth rates: Although the growth rates from visual and pitot measurements lie within the rather large

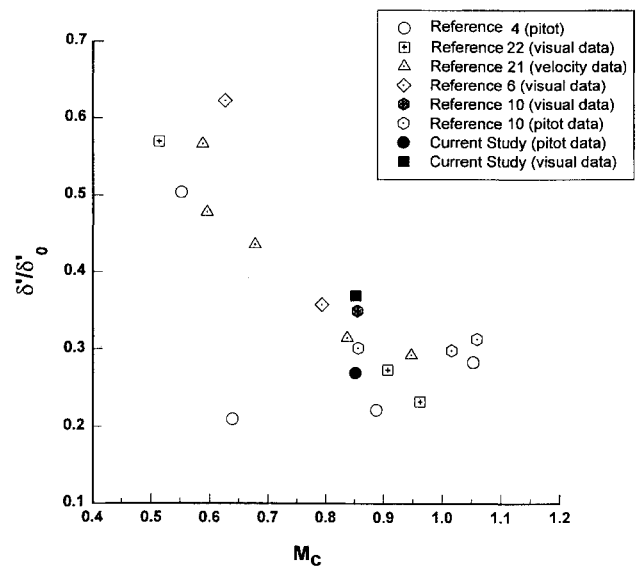

Fig. 7 Normalized growth rate of compressible shear layers.

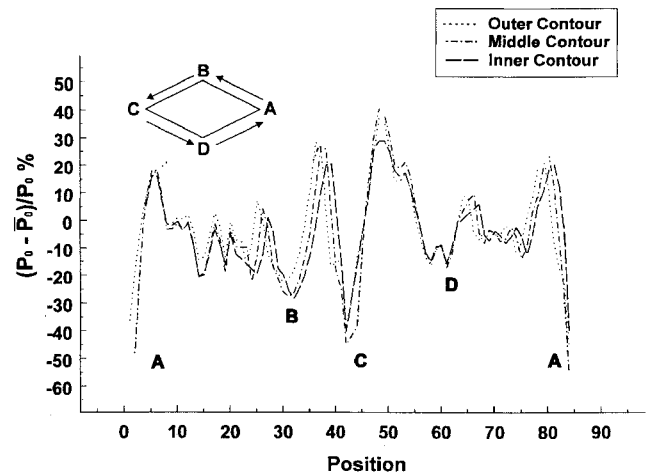

Fig. 8 Pitot profile along a diamond contour at $x/h = 2$ (numbers on the x axis represent position along the contour) showing evidence of streamwise vorticity.

scatter of published data, the pitot growth rate extracted from visual data was approximately 30% higher than the corresponding rate deduced from pitot surveys. This discrepancy is likely because the scaling factor of 0.72, used to convert visual thickness to pitot thickness, is based primarily upon visual measurements using schlieren images; because the current visual data relied on PLS images, a scaling factor of 0.72 may not be as appropriate.

D. Shear-Layer Vortical Structures

The presence of streamwise vorticity, distinctly suggested in the PLS images, was further investigated via additional pitot measurements. This was accomplished by conducting pitot surveys along the shear layer in the shape of the nozzle contour (a diamond-shaped locus of points) at various streamwise locations. At each location, the diamond-contour pitot surveys were conducted in three regions of the shear layer in the following manner: an inner survey, near the high-speed edge of the shear layer; a survey along the middle of the shear layer; and an outer contour survey closer to the low-speed edge of the shear layer. These surveys may then be used to verify the stationarity and the cross-stream extent of the streamwise structures. A profile at $x/h = 2$ is plotted in Fig. 8.

The four corners of the diamond, marked as A, B, C, and D, correspond to the locations in the sketch of nozzle contour shown in the inset. To accentuate the fluctuations in the pitot pressures, the average value of the pitot pressure along the nozzle contour, $\bar{P}_0$, is subtracted from the local pitot pressure P_0, and the reduced pressure

$(P_0 - \bar{P}_0)$ is expressed as a percentage of the local pitot pressure. The value $(P_0 - \bar{P}_0)/P_0\%$, which represents the percentage variation of the local pitot pressure, is plotted in the ordinate. Because the length of the perimeter of a contour survey depends upon the part of the shear layer—inside, middle, or outside—in which the survey is conducted, the total distance traversed by the probe in a given survey is divided into 90 equally spaced points. Hence, each number shown on the abscissa in Fig. 8 represents the same relative measurement location along the nozzle contour in all three parts of the shear layer.

The pitot profiles display four primary pressure valleys or minima and multiple smaller undulations (secondary maxima and minima). The primary minima in the vicinity of the jet corners roughly correspond to the location of the large structures, observed near the jet vertices in the PLS images of Fig. 4. Similar pitot profiles and visual evidence of structures along the shear-layer periphery have been obtained by others in shear layers of underexpanded jets.[11–13] Zapryagaev and Solotchin[13] proposed that the peaks and valleys in the pitot profiles and the indentations in the PLS images are attributable to the presence of pairs of counter-rotating vortices along the periphery of the jet. Depending upon the sense of rotation of the vortex pairs, they either expel high-pressure, cold jet fluid into the surroundings or entrain low-pressure, warm ambient fluid, resulting in pressure peaks and valleys and ripples in the PLS images. (A more detailed discussion of the connection between the vortical structures and the observed behavior can be found elsewhere.[11–13]) Because of the remarkable similarity between the present measurements and the references cited earlier, in addition to the fact that one would expect significant streamwise vorticity to be generated at the nozzle corners, we believe that the primary pressure minima and the large structures in Fig. 4 signify the presence of pairs of counter-rotating vortices at each of the nozzle corners. If this is indeed the case, we expect the strength of these vortices to be inversely proportional to the included angle at the diamond jet corners. The profiles in Fig. 8 support this hypothesis because the pressure difference between the adjacent maxima and minima is significantly higher at A and C.

A more intriguing and rather unexpected feature of these profiles is the presence of localized secondary maxima and minima in the shear layers in regions away from the corners. A close examination of Fig. 8 reveals the presence of six to eight secondary peaks in the pitot pressures. These secondary pressure features, concomitant with the appearance of secondary corrugated structures or ripples observed in Fig. 4, once again suggest that these structures are a result of counter-rotating vortices in the periphery of the shear layer. The smaller magnitude of the secondary features indicates that, these vortices are much weaker than the corner vortices discussed earlier. Whereas the presence of streamwise vorticity at the jet vertices is relatively easily explained, at least from a phenomenological perspective, the source of the secondary structures is not readily evident and merits further discussion.

As mentioned earlier, similar behavior signifying the presence of streamwise vortices has been observed by other researchers.[11–13] However, in each of those studies the streamwise vortices were only generated in underexpanded jets. This observation led the investigators to suggest that the vortices were a result of a Taylor–Goertler type instability attributable to the concave curvature (bulging out) of the shear layer of underexpanded jets. In a more recent study, King et al.[14] discovered that jet curvature or a Taylor–Goertler type instability was not a necessary condition for the generation of streamwise vorticity. By providing three-dimensional disturbances in the nozzle boundary layer, they were able to generate similar structures in the shear layers of ideally expanded jets. King et al.[14] proposed that although a Taylor–Goertler instability may elevate the amplification rates of disturbances, a finite-amplitude three-dimensional input, such as that created by scratches on the nozzle surface, is necessary to generate significant streamwise vorticity. (Note that two-dimensional disturbances did not trigger the formation of vortices.)

The diamond jet in the present study was operated at ideally expanded conditions, which rules out the possibility of the Taylor–Goertler instability for producing the streamwise vorticity. Furthermore, the EDM technique used to fabricate the nozzle yields a very smooth surface, and a close scrutiny of the nozzle surface revealed no surface imperfections. In the absence of shear-layer curvature

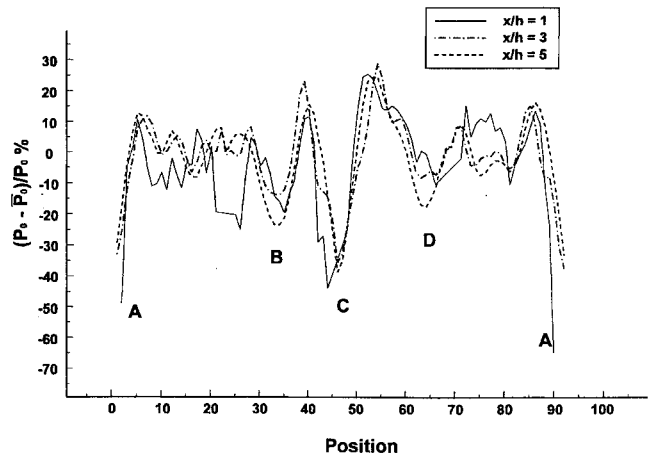

Fig. 9 Diamond contour pitot profiles (numbers on the x axis represent position along the contour) showing streamwise evolution of vortical structures.

and three-dimensional disturbance input at the nozzle surface, one must look elsewhere for the source of the significant vorticity that is clearly present in this flowfield. We suggest that such disturbances may be present in the nozzle boundary layer. A likely candidate for a disturbance source would be the region where the nozzle geometry transitions from an axisymmetric to a diamond shape. Despite the smooth transition, it is likely to produce three-dimensional, secondary flows near the throat of the nozzle and in the developing boundary layer. These disturbances may then serve as the necessary input for the streamwise vorticity observed downstream. We recognize that the evidence of streamwise vorticity, based on flow visualization and pitot measurements alone, is circumstantial in nature. However, such measurements have been used by other researchers as proof of streamwise vorticity.[11–13] Strictly speaking, presence of streamwise vorticity can only be conclusively demonstrated via direct velocity measurements, which are very difficult to make in supersonic flows using conventional techniques such as hot wires. We are attempting to make these measurements using particle image velocimetry and, if successful, we will present the results in a subsequent paper.

The spatially stationary character of these structures is clearly evident from the very good overlap of the three pitot profiles along the inner, middle, and outer parts of the shear layer, as seen in Fig. 8. Another notable feature is the spatial evolution of these vortices with downstream distance. To understand this behavior, we examine Fig. 9, which shows diamond-contour pitot surveys conducted at four streamwise locations. Each survey is conducted in the middle of the shear layers. The strong disturbances at the jet corners remain the dominant features at all streamwise positions, up to and including the farthest downstream location ($x/h = 5$). The relative magnitude of the primary peaks decreases slightly while their spatial extent increases moderately with streamwise distance. In contrast, the secondary maxima and minima evolve more rapidly as one progresses downstream. Whereas 8–10 secondary peaks are evident in the profile at $x/h = 1$, only 4–5 are present at the farthest downstream station. A closer examination of the profiles shows a broadening and merging of neighboring secondary peaks with downstream distance. This indicates that the smaller vortices are merging into larger ones as the flow develops, a trend also perceived in the PLS images of Fig. 4. The merging of neighboring vortices has also been observed by other investigators.[11–13] Unfortunately, no pitot surveys were conducted beyond $x/h = 5$; however, by examining the PLS image in Fig. 4, one may easily speculate that at some downstream location, the disturbances at the jet corners would engulf the smaller vortices along the straight edges of the jet and would thus be the only discernible features in the pressure profiles.

E. Noise Characteristics

In this section, we discuss the acoustic properties of the present flowfield, which were explored in some detail. Our primary intent is to examine the effect of the nozzle geometry and the apparent

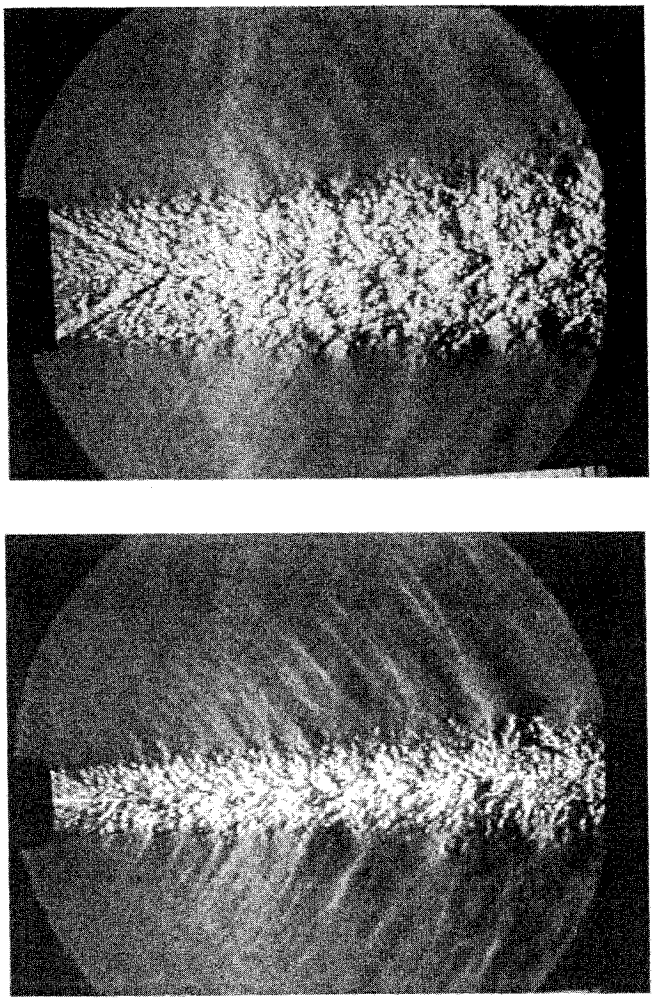

Fig. 10 Instantaneous schlieren image depicting Mach wave radiation.

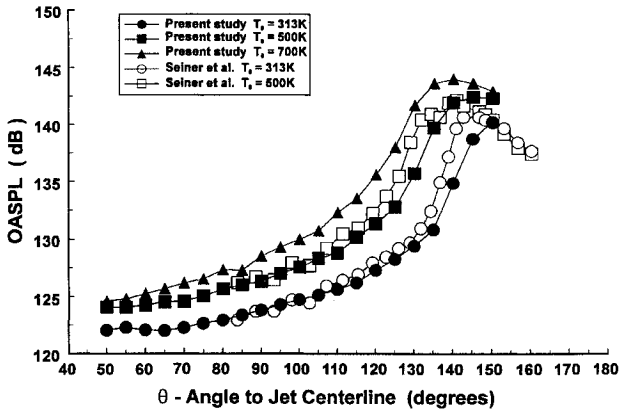

Fig. 11 Angular variation of OASPL of a Mach 2 axisymmetric jet.

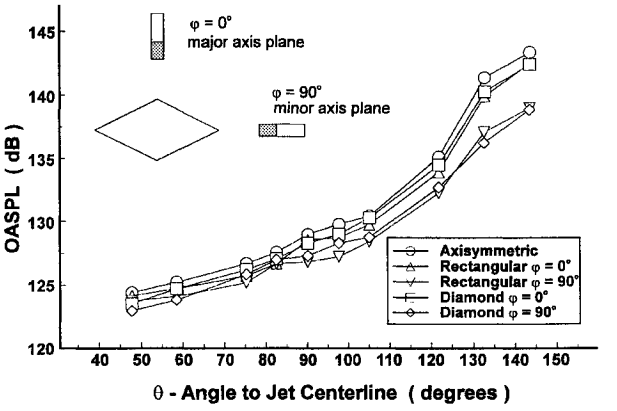

Fig. 12 Angular variation of OASPL, showing axisymmetric, rectangular, and diamond jets (T_0 = 700 K).

presence of streamwise vorticity on far-field mixing noise (shock-associated noise is not relevant because the jet is operating at design conditions).

Typical schlieren pictures of the jet in the two orthogonal central planes containing the short and long dimensions of the nozzle are shown in Fig. 10. These pictures demonstrate the wave-free flow attained using this nozzle. Strong directional acoustic radiation, attributable to Kelvin–Helmoltz instability waves in the shear layer, is clearly seen in the ambient environment. Such a wave system is commonly referred to as Mach wave radiation, properties of which have been discussed elsewhere.[15] These waves propagate outward at a Mach emission angle of about 39 deg, in accord with the measurements of Wishart[16] for a corresponding axisymmetric jet. The agreement of the emission angle and the wavelength of the radiation field with those of an axisymmetric jet suggests that the nozzle exit geometry and the resulting streamwise vorticity do not significantly affect the dominant Kelvin–Helmoltz type instability of the shear layer.

To establish the reliability of the acoustic measurements, we first compare the data taken in the present facility with previous experiments. Because no acoustic data for diamond-shaped jets are available in literature, the data for a Mach 2 axisymmetric jet, taken in the anechoic facility, are compared to the extensive measurements of Seiner et al.,[17,18] as shown in Fig. 11. The OASPL, taken in a circular arc at a radial distance of about 40 diameters at various θ (see Fig. 2), is plotted in this figure for three different stagnation temperatures. Under similar conditions, the two sets of measurements agree reasonably well. Any differences in the data may be attributed to the different ambient conditions in the respective anechoic chambers. The data of Seiner et al.[17] were obtained with a linear array and subsequently corrected to a circular arc, whereas the present data were taken along a circular arc centered at the nozzle exit. In addition, the diameter of the nozzles used by Seiner et al.[17] was five times larger than the one used in this investigation.

The dominant part of the noise is confined to the aft quadrant at angles greater than 100 deg (the region defined by $\theta = 0$–90 deg is usually referred to as the forward quadrant, whereas the region bounded by $\theta = 90$–180 deg is referred to as the aft quadrant). In the upstream direction, the noise intensity is low and relatively independent of the direction. With increasing stagnation temperature, the overall noise radiation increases, as shown in Fig. 11. These results are in accord with the present understanding of the turbulent mixing noise of supersonic jets described by Tam.[2]

The effect of nozzle exit geometry on the far-field noise is shown in Fig. 12. In addition to the axisymmetric and diamond nozzle configurations, an equivalent rectangular Mach 2 C–D nozzle (aspect ratio = 4) was used. One of the principal characteristics of the radiation field of a noncircular jet is its dependence on the plane of measurement with respect to the nozzle exit. For example, Seiner and Ponton[19] observed that a significant noise reduction in the minor axis plane of an elliptic jet can be observed when compared to an equivalent axisymmetric jet. A comprehensive discussion of the noise radiation from noncircular supersonic jets is given by Morris.[20] The variation of the OASPL with the angle to the inlet axis is shown in Fig. 12 for a heated jet (T_0 = 700 K). The data for noncircular jets were taken in the two central major- and minor-axes planes of the nozzle as shown in the figure (see inset). Significant noise reduction (about 5 dB) was observed in the aft quadrant (Fig. 12) for the minor-axis plane of the diamond and rectangular jets as compared to an axisymmetric jet, but no meaningful reduction was observed in the major-axis plane. Although only data for a heated jet are shown in Fig. 12, similar trends, with less noise reduction, are observed for the cold jet. Such observations are consistent with results of elliptic jets.[19] These results indicate that the presence of streamwise vorticity in the diamond jet has minimal influence on the far-field OASPL.

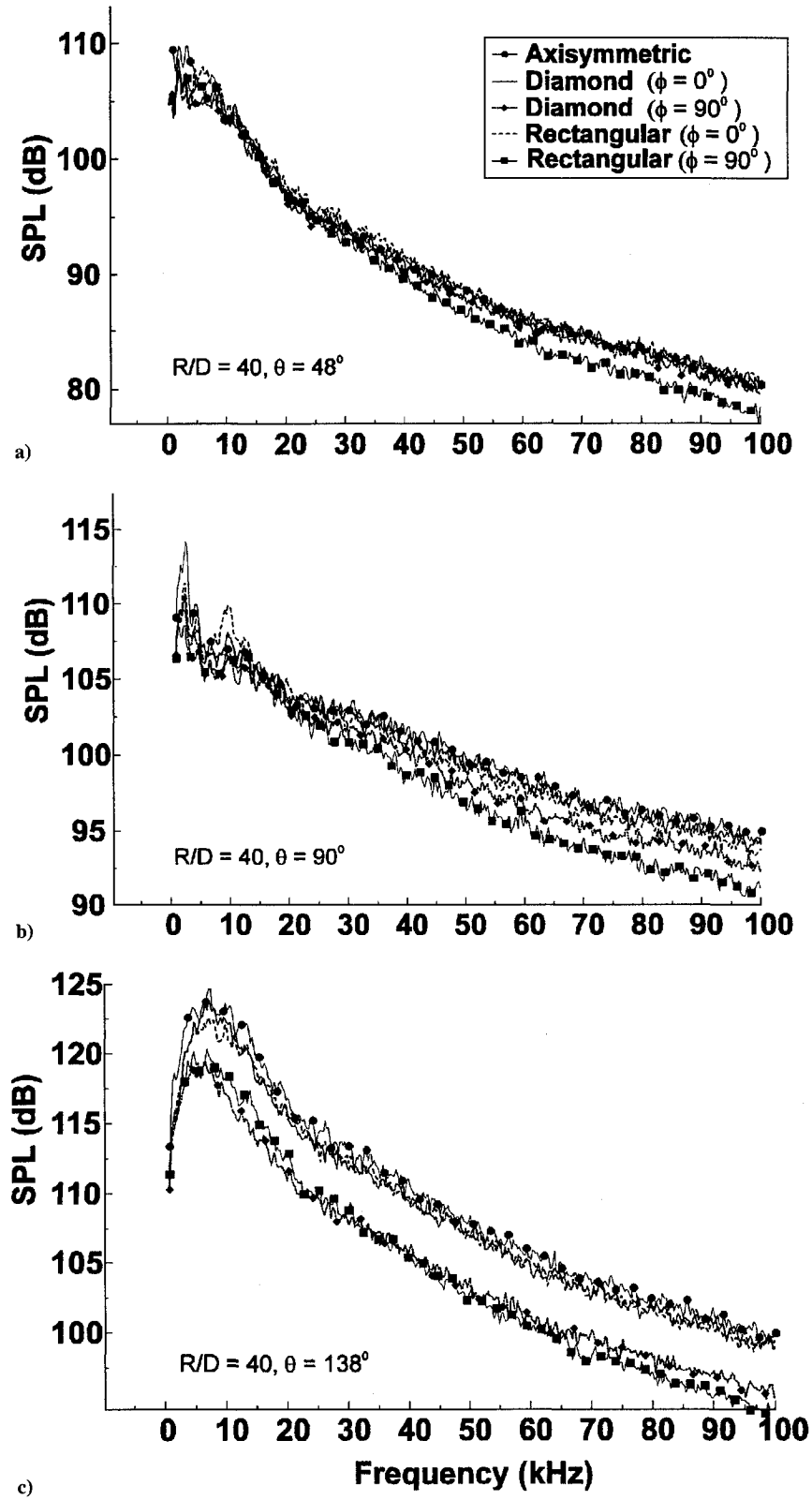

Fig. 13 Power spectra of axisymmetric, rectangular, and diamond jets (T_0 = 700 K).

Far-field narrow-band noise spectra were also obtained to investigate any frequency shifts that may occur because of different nozzle exit geometry. Typical spectra, representative of forward and aft quadrants and normal to the jet axis, are shown in Figs. 13a and 13b for heated jets (θ = 48 and 138 deg were the maximum angles in the forward and aft quadrants along which measurements could be made without wall interference). Included are the data for a rectangular jet operating under identical conditions. As shown in Fig. 13c, reduction of SPL in the aft quadrant occurs at all frequencies in the spectrum for both the diamond and the rectangular nozzles, in the plane of the short dimension. In contrast, only minor changes in the amplitude of the spectrum are observed in the other two directions. The peak Strouhal number Sr for the mixing noise in the aft quadrant falls within a range of 0.24–0.26 and seems to be independent of nozzle geometry.

IV. Concluding Remarks

The aerodynamic and acoustic properties of a diamond-shaped jet are explored in this paper. The pitot surveys and the flow visualization study show the presence of distinct structures in the shear layers.

On the basis of their remarkable similarity to the features observed by other investigators, we propose that they represent convincing evidence of substantial streamwise vorticity in the shear layer. Such streamwise vorticity is not normally observed in the shear layers of two-dimensional and axisymmetric jets operating under ideally expanded conditions. A possible mechanism for the generation of this vorticity has been suggested. Interestingly enough, though the turbulent and mean flowfield structure of the present shear layer is very different from the shear layers generated by axisymmetric and rectangular jets, the global growth rates of the shear layer agree exceptionally well with its two-dimensional and axisymmetric counterparts. This suggests that even though streamwise vorticity may affect the shear layer locally, e.g., by increasing the local thickness of the shear layer, the global growth rate is still primarily determined by global parameters characterizing the shear layer, such as the velocity ratio, the density ratio, and the convective Mach number.

The far-field noise properties of the diamond jet also have been studied utilizing narrow-band spectra. In selected planes of the diamond jet, a moderate reduction (5 dB) of mixing noise of hot jets was observed as compared to that of an equivalent axisymmetric jet. Such a reduction, observed in the aft quadrant, becomes less significant at lower stagnation temperatures. Given the fact that this nozzle geometry generates a jet with significant streamwise vorticity, it has an apparently minor effect on the far-field noise. Any reduction in the mixing noise observed in the far field seems to be associated with the orientation of the jet column with respect to the measurement plane. From these experiments, it may be suggested that the presence of streamwise vorticity in ideally expanded supersonic jets has very little effect on the aerodynamic and noise fields of the jet.

Acknowledgments

We gratefully acknowledge the support of NASA (NAG 2930) in conducting this research. We also thank Paul Strykowski of the University of Minnesota for the enlightening discussions during this investigation and Edward Barber for his assistance in conducting the experiments.

References

[1]Tam, C. K. W., "Jet Noise Generated by Large-Scale Coherent Motion," *Aeroacoustics of Flight Vehicles: Theory and Practice*, NASA RP-1258, Vol. 1: Noise Source, 1991, pp. 311–390.

[2]Tam, C. K. W., "Supersonic Jet Noise," *Annual Review of Fluid Mechanics*, Vol. 27, 1995, pp. 17–43.

[3]Brown, G. L., and Roshko, A., "On Density Effects and Large Structure in Turbulent Mixing Layers," *Journal of Fluid Mechanics*, Vol. 64, No. 4, 1974, pp. 775–781.

[4]Papamoschou, D., and Roshko, A., "The Compressible Turbulent Shear Layer; An Experimental Study," *Journal of Fluid Mechanics*, Vol. 197, Dec. 1988, pp. 453–477.

[5]Clemens, N. T., and Mungul, M. G., "Two- and Three-Dimensional Effects in the Supersonic Mixing Layer," *AIAA Journal*, Vol. 30, No. 4, 1992, pp. 973–981.

[6]Shau, Y. R., Dolling, D. S., and Choi, K. Y., "Organized Structure in a Compressible Turbulent Shear Layer," *AIAA Journal*, Vol. 31, No. 8, 1993, pp. 1398–1405.

[7]Krothapalli, A., King, C. J., and Strykowski, P. J., "The Role of Streamwise Vortices on Sound Generation of a Supersonic Jet," AIAA Paper 93-4320, Oct. 1993.

[8]Hawkins, R., and Hoch, R., "Studies into Concorde's Engine Noise Emission," 10th International Aeronautical Congress, Paris, France, June 1971.

[9]Pannu, S. S., and Johannesen, N. H., "The Structure of Jets from Notched Nozzles," *Journal of Fluid Mechanics*, Vol. 74, April 1976, pp. 515–528.

[10]Strykowski, P. J., Krothapalli, A., and Jendoubi, S., "The Effect of Counterflow on the Development of Compressible Shear Layers," *Journal of Fluid Mechanics*, Vol. 308, Feb. 1996, pp. 63–96.

[11]Krothapalli, A., Buzyna, G., and Lourenco, L., "Streamwise Vorticies in an Under-Expanded Axisymmetric Jet," *Physics of Fluids A*, Vol. 3, No. 8, 1991, p. 1848.

[12]Arnette, S. A., Samimy, M., and Elliott, G. S., "On Streamwise Vortices in High Reynolds Number Supersonic Axisymmetric Jets," *Physics of Fluids A*, Vol. 5, No. 1, 1993, p. 187.

[13]Zapryagaev, V. I., and Solotchin, A. V., "Spatial Structure of Flow in the Initial Section of a Supersonic Under-Expanded Jet," Academy of Sciences USSR, Siberian Section, Inst. of Theoretical and Applied Mechanics, Preprint No. 23-88, UDK 533.6.011, 1988.

[14]King, C. J., Krothapalli, A., and Strykowski, P. J., "Streamwise Vorticity Generation in Supersonic Jets with Minimal Thrust Loss," AIAA Paper 94-0661, Jan. 1994.

[15]Tam, C. K. W., "Directional Acoustic Radiation Generated by Shear Layer Instability," *Journal of Fluid Mechanics*, Vol. 46, April 1971, pp. 757–768.

[16]Wishart, D. P., "The Structure of a Heated Supersonic Jet Operating at Design and Off-Design Conditions," Ph.D. Dissertation, Dept. of Mechanical Engineering, Florida State Univ., Tallahassee, FL, April 1995.

[17]Seiner, J. M., Ponton, M. K., Jansen, B. J., and Lagen, N. T., "The Effects of Temperature on Supersonic Jet Noise Emission," DGLR/AIAA 14th Aeroacoustics Conf., Paper 92-02-046, Aachen, Germany, 1992.

[18]Seiner, J. M., and Ponton, M. K., "Aeroacoustic Data for High Reynolds Number Supersonic Axisymmetric Jets," NASA TM-86296, 1985.

[19]Seiner, J. M., and Ponton, M. K., "Supersonic Acoustic Source Mechanisms for Free Jets of Various Geometries," AGARD 78th B Specialists Meeting, Paper 16, Bonn, Germany, Oct. 1991.

[20]Morris, P. J., "Noise Radiation from Non-Circular Supersonic Jets," DGLR/AIAA 14th Aeroacoustics Conf., Paper 92-02-061, Aachen, Germany, 1992.